

# Effect of Multiwall Carbon Nanotube and Au Nanoparticle on the Structure–Property Relationship of Poly(*N*-isopropyl acrylamide)

R. Anbarasan,<sup>1</sup> C. A. Peng<sup>2</sup>

<sup>1</sup>Department of Polymer Technology, Kamaraj College of Engineering and Technology, Virudhunagar 626 001, Tamil Nadu, India

<sup>2</sup>Department of Chemical Engineering, Nano-biotechnology Research Lab, National Taiwan University, Taipei 10617, Taiwan, Republic of China

Received 17 May 2010; accepted 22 January 2011

DOI 10.1002/app.34219

Published online 29 November 2011 in Wiley Online Library (wileyonlinelibrary.com).

**ABSTRACT:** Temperature-sensitive poly(*N*-isopropyl acrylamide) (PNIPAAm) was synthesized both in the presence and absence of nanomaterials like allyl mercaptan decorated gold nanoparticle and allyl alcohol-conjugated multiwall carbon nanotube. The influence of the nanomaterials on the structure–property relationship of PNIPAAm was analyzed and critically compared to the pristine PNIPAAm. During the *in situ* polymerization, the nanosphere shape of Au nanoparticle was converted into Au nanorod shape, which

was confirmed through UV–vis spectroscopy. The glass transition temperature ( $T_g$ ) of polymer/nanocomposites was greater than that of the pristine polymer. Thermogravimetric analysis declared that the polymer/nanocomposites exhibited higher thermal stability than the homopolymer. © 2011 Wiley Periodicals, Inc. *J Appl Polym Sci* 124: 3996–4006, 2012

**Key words:** poly(*N*-isopropyl acrylamide); FTIR; DSC; TGA; XPS; SEM

## INTRODUCTION

Polymeric hydrogel-like poly(*N*-isopropyl acrylamide) (PNIPAAm) is the most studied thermoresponsive polymers and exhibits wide range of applications in various science and biomedical engineering field, particularly in drug-delivery systems.<sup>1–5</sup> Such a thermal responsive polymer's structures are altered in the presence of foreign impurities like nanomaterials. Stile and coworkers<sup>6</sup> reported the synthesis and characterizations of PNIPAAm homopolymer and its copolymer. The PNIPAAm copolymers were synthesized and its acute and subacute toxicity in mice was tested.<sup>7</sup> Poly(citraconic acid)-grafted PNIPAAm was synthesized and its drug releasing properties were tested by Tasdelen et al.<sup>8</sup> Wu and coworkers<sup>9</sup> studied the lower critical solution temperature of PNIPAAm in an aqueous medium. Core-shell microgels of PNIPAAm/poly(vinyl alcohol) were synthesized and characterized by zeta potential, scanning electron microscopy (SEM), transmission electron microscopy (TEM), nuclear magnetic resonance spectroscopy (NMR), and turbidity measurements.<sup>10</sup> Other authors also reported about the synthesis and characterizations of PNIPAAm.<sup>11–25</sup> By thorough literature survey, we could not find any

report based on the copolymerization of vinyl functionalized nanomaterials like Au and multiwall carbon nanotube (MWCNT) with *N*-isopropylacrylamide (NIPAAm) in the presence of peroxydisulphate (PDS) as a free radical initiator. In the present investigation, we took this job as a challenge and successfully synthesized the same and characterized with different analytical tools like Fourier transform infrared spectroscopy (FTIR), UV–vis spectroscopy, differential scanning calorimetry (DSC), thermogravimetric analysis (TGA), photoluminescence spectroscopy (PL), X-ray photoelectron spectroscopy (XPS), SEM and TEM.

## EXPERIMENTAL

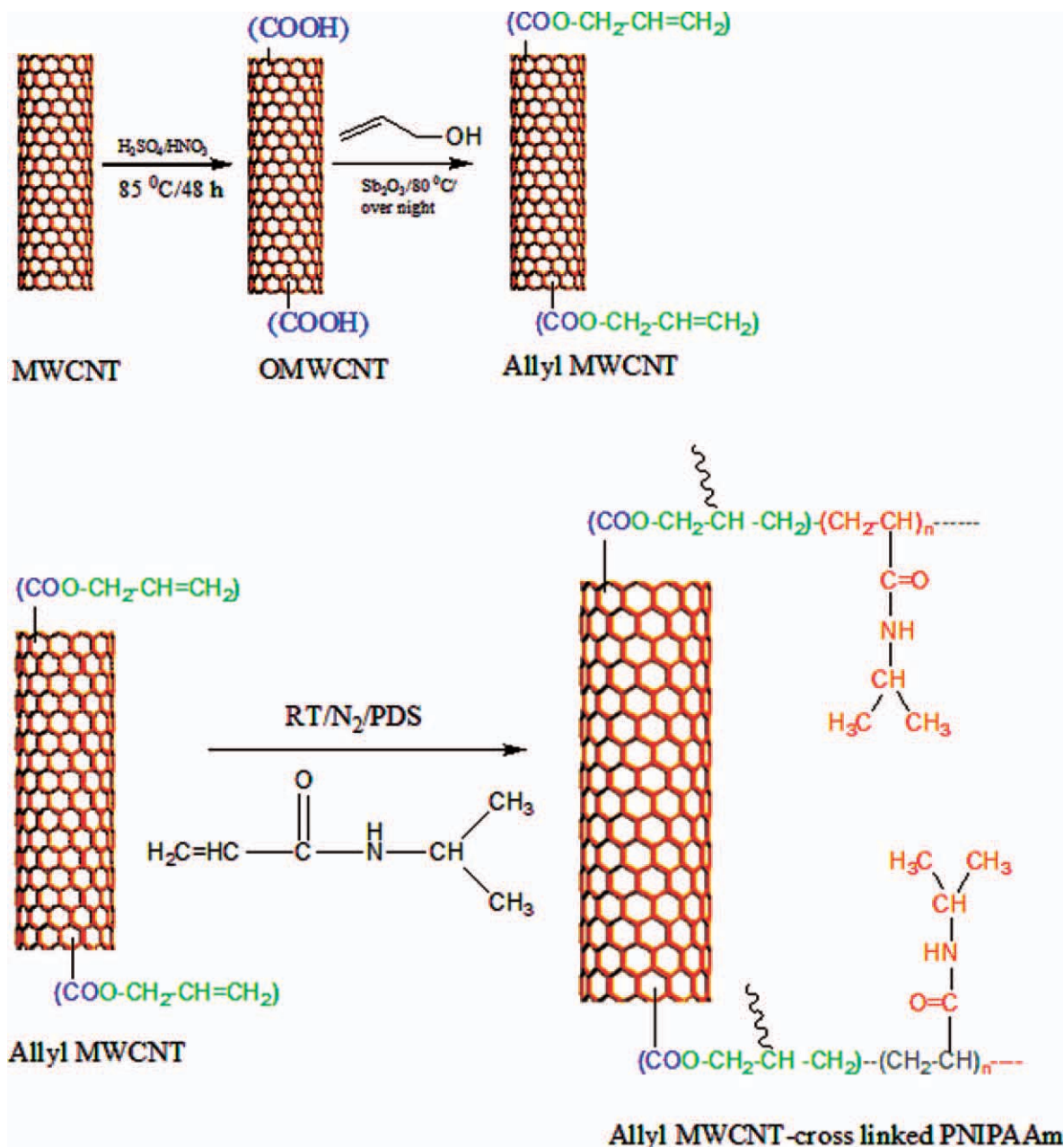
### Materials

NIPAAm (Aldrich, USA) was purified by recrystallization from *n*-hexane solvent. PDS (Across, USA), chloroauric acid (HAuCl<sub>4</sub>, Across), sodium borohydride (NaBH<sub>4</sub>, Showa Chemicals, Japan), allylmercaptan (AM, Across), and allyl alcohol (AA, Across) were received and used as such. MWCNT (CNT company, Taiwan), antimony oxide (Sb<sub>2</sub>O<sub>3</sub>, Showa chemicals, Japan), and ethanol (Showa chemicals) were used without further purification.

### Synthesis of oxidized multiwalled carbon nanotube

About 0.10 g of multiwalled carbon nanotube (MWCNT) was taken in a 250-mL beaker and charged

Correspondence to: R. Anbarasan (anbu\_may3@yahoo.co.in).



**Scheme 1** [Color figure can be viewed in the online issue, which is available at [wileyonlinelibrary.com](http://wileyonlinelibrary.com).]

with 10 mL of Con. $\text{H}_2\text{SO}_4$  and 10 mL of Con. $\text{HNO}_3$ . About 100 mL of double-distilled water (DDW) was added and heated up to  $85^\circ\text{C}$  for 48 h under vigorous stirring condition. At the end of the reaction time, the edge-oxidized products were repeatedly washed with water to remove the excess acid and dried under vacuum freeze drier. Thus, obtained fine powders of oxidized multiwalled carbon nanotube (OMWCNT) were weighed and stored in a zipper bag (yield-90%). The reactions are represented in Scheme 1.

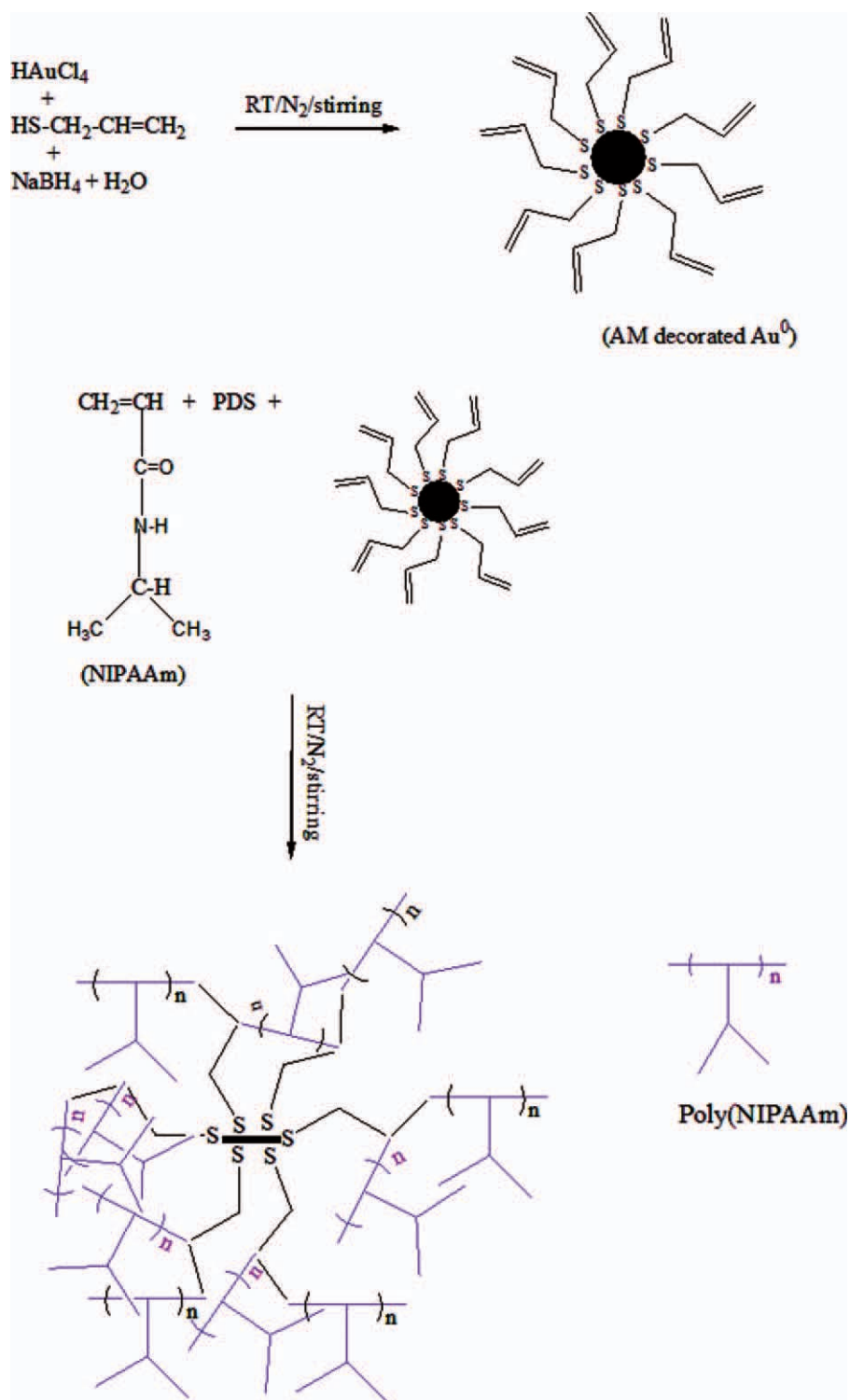
#### Synthesis of allylated MWCNT

About 0.05 g of edge-oxidized multiwalled carbon nanotube (MWCNT) was dispersed in 50 mL of

DDW under ultrasonication for 1 h at room temperature. About 5 mL of AA was added drop wise to the content under mild stirring condition. About 0.03 g of  $\text{Sb}_2\text{O}_3$ , condensation catalyst was added, and the reaction temperature was raised to  $80^\circ\text{C}$ . The dark black product was centrifuged and repeatedly washed with water after 6 h of reaction. The purified products were obtained after freeze drying, and the yield was noted as 85% and stored in a zipper bag. The reaction is shown in Scheme 1.

#### Synthesis of gold nanoparticles (Au NP)

About 1 mL of  $\text{HAuCl}_4$  was taken in a 100-mL double-necked round-bottomed flask (RBF) already



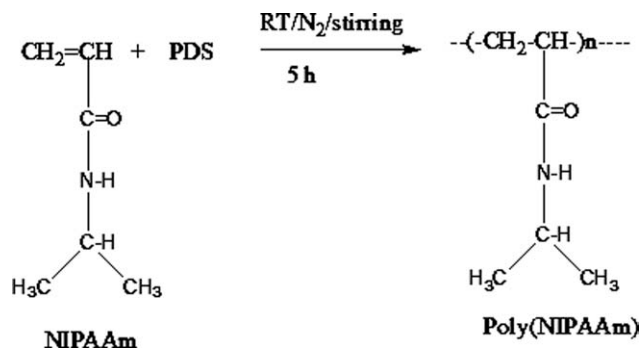
**Scheme 2** [Color figure can be viewed in the online issue, which is available at [wileyonlinelibrary.com](http://wileyonlinelibrary.com).]

charged with 25 mL of DDW and the nitrogen gas was passed into the solution. The cold  $\text{NaBH}_4$  solution (0.50 g/25 mL DDW) was added drop wise with the help of syringe for 30 min. Then, 5 mL of AM was syringed into the RBF, and the stirring was continued for another 2 h. The brown precipitate was filtered and freeze dried. Thus, obtained dark

brown crystals are AM decorated Au NP. Scheme 2 represents the reaction.

#### Synthesis of PNIPAAm homopolymer and its copolymers

About 25 mL of 0.1M *N*-isopropyl acrylamide (NIPAAm) monomer solution was taken in a



double-necked RBF. The solution was purged with pure nitrogen gas for 30 min under mild stirring condition. About 10 mL of 0.01M PDS solution was added drop wise for 30 min at room temperature. Then, the stirring was allowed for another 5 h with nitrogen purging. After 5 h of homopolymerization reaction, the contents were filtered and dried by using freeze drier. After 48 h of freeze drying, fine powders of PNIPAAm were obtained and stored in a zipper bag. Reactions are shown in Scheme-3.

Under the same experimental conditions, copolymers of NIPAAm were prepared. For example, 10 mg of AA-MWCNT was dispersed in 5 mL of DMF and added with the monomer solution under vigorous stirring condition at room temperature (Scheme 1). The remaining procedure is similar to that of the synthesis of homo PNIPAAm. In the case of Au NP, more than 1 AM. monomer was adsorbed on the surface of Au NP through the mercaptyl group. Hence, there is a chance for the crosslinking reaction. About 10 mg of AM decorated Au NP was mixed with the NIPAAm monomer, and the copolymerization was carried out as mentioned earlier (Scheme 2). During the copolymerization reaction, some amount of homopolymer of PNIPAAm was also formed. In Scheme 1, the formation of homopolymer is not indicated. The homopolymer formation is separately mentioned in Scheme 3. Schemes 1–3 are proposed here based on the FTIR, TEM, UV–vis spectroscopy and TGA results.

### Characterizations

FTIR spectra for the samples were recorded with the help of Perkin–Elmer Spectrum 100 series instrument by KBr pelletization method from 400 to 4000  $\text{cm}^{-1}$ . Jasco V-570 instrument was used for UV–vis spectrum measurements. DSC was measured by using Universal V4.4A TA Instruments under nitrogen atmosphere at the heating rate of 10°C/min from room temperature to 200°C. The second heating scan of the sample was considered to delete the

previous thermal history of the sample. TGA was conducted in air atmosphere on a Rigagu TGA 8120 instrument from 30 to 500°C at the heating rate of 10°C/min. Photoluminescence spectrum (PLS) was measured with the help of PL, Jasco Model FP-6000, Japan, instrument from 400 to 700 nm. SEM of PNIPAAm samples were recorded with the help of JSM 6300, Jeol product, instrument. The binding energy of PNIPAAm systems was determined by XPS (XPS, Thermo Scientific, Theta Probe, UK). TEM was recorded with the help of TEM 3010, JEOL, and Japan Instrument.

## RESULTS AND DISCUSSION

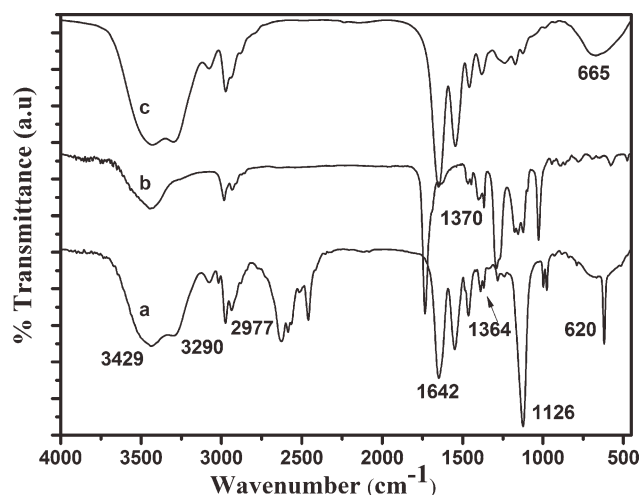
For the sake of convenience, the results and discussion part is subdivided into two parts namely, (1) synthesis and characterizations of PNIPAAm-AM-Au copolymer systems and (2) synthesis and characterizations of PNIPAAm-AA-MWCNT systems. Even though the gold nanoparticles and MWCNT are having nanosize, their role on the nanocomposite formation with PNIPAAm is entirely different from each other. Hence, it is necessary to study the influence of such nanomaterials on the structure–property relationship of PNIPAAm separately.

The above study indicates that all the nanomaterials are not having same type of effect on the structure property relationship of PNIPAAm. The Au NP is in sphere form, whereas the MWCNT is in tube form, so that we cannot compare its influence on the structure–property relationship of PNIPAAm. In the case of Au NP, the vinyl monomers are adsorbed on the surface of Au NP, whereas in the case of MWCNT, the vinyl monomers are chemically interacted with MWCNT. Hence the results and discussion part is subdivided into two parts.

### Synthesis and characterizations of PNIPAAm-AM-Au copolymer systems

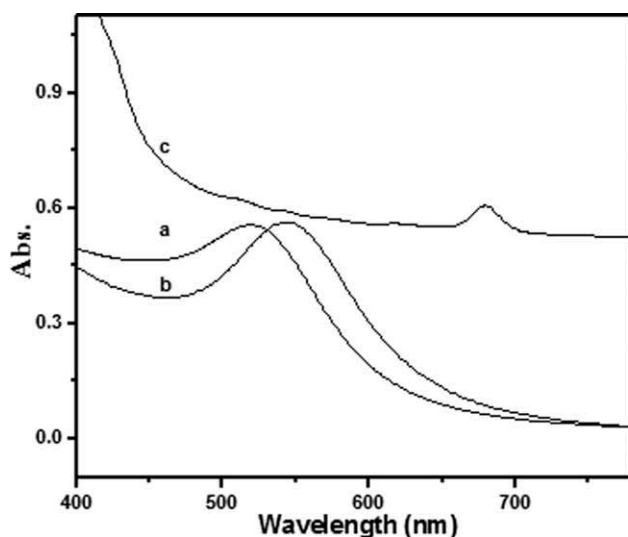
#### FTIR study

Figure 1(a) indicates the FTIR spectrum of pristine poly(*N*-isopropyl acrylamide) (PNIPAAm). A broad peak at 3429  $\text{cm}^{-1}$  is due to the OH stretching of water molecules associated with the PNIPAAm. A hump at 3290  $\text{cm}^{-1}$  is responsible for the N–H stretching of PNIPAAm. The C–H symmetric and antisymmetric stretching is observed at 2938 and 2977  $\text{cm}^{-1}$  respectively. Peak around 2500  $\text{cm}^{-1}$  is accounted by the carbonate stretching. Peaks at 1642 and 1364  $\text{cm}^{-1}$  are due to the C=O and C–N stretching of PNIPAAm, respectively. The C–O–N and C–H out of plane bending vibrations of PNIPAAm are observed at 1126 and 620  $\text{cm}^{-1}$ , respectively. Figure 1(b) indicates the FTIR spectrum of



**Figure 1** FTIR spectra of (a) PNIPAAm, (b) AM decorated Au NP, (c) PNIPAAm-AM-Au.

AM decorated Au NP. The O—H ( $3438\text{ cm}^{-1}$ ), C—H symmetric ( $2922\text{ cm}^{-1}$ ), C—H antisymmetric ( $2982\text{ cm}^{-1}$ ), carbonyl stretching ( $1725\text{ cm}^{-1}$ ), C—S stretching ( $1370\text{ cm}^{-1}$ ), and Au—S (M-S) stretching ( $572\text{ cm}^{-1}$ ) are observed. This confirmed the decoration of Au NP by AM. In this case, the carbonyl stretching at  $1725\text{ cm}^{-1}$  is due to the atmospheric carbonate interaction. The amide carbonyl stretching of PNIPAAm is appeared at the lower wave number ( $1642\text{ cm}^{-1}$ ). Figure 1(c) represents the FTIR spectrum of PNIPAAm-AM-Au system. The important peaks are characterized below: The C-S and M-S stretching are observed at  $1375$  and  $665\text{ cm}^{-1}$ , respectively. The other peaks are corresponding to the PNIPAAm. Appearance of C-S and M-S stretching confirmed the presence of AM-Au in the PNIPAAm matrix as a comonomer.



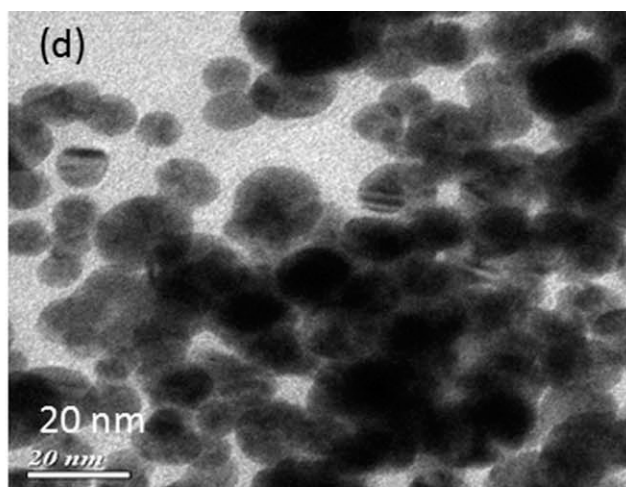
**Figure 2** UV-vis spectrum of (a) Au NP, (b) AM decorated Au NP, (c) PNIPAAm-AM-Au, and (d) TEM image of pristine Au nanoparticle.

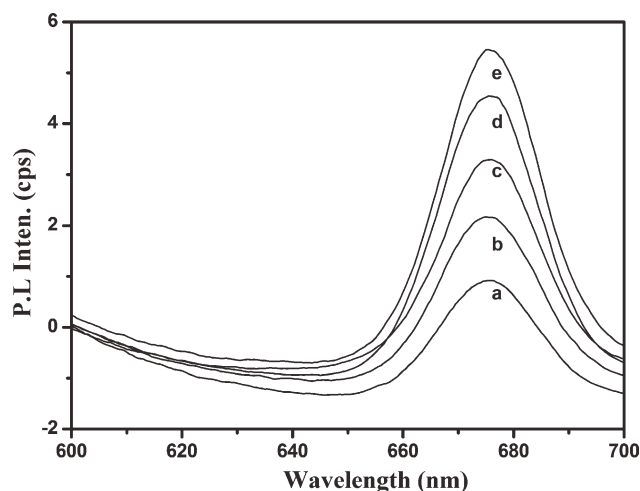
#### UV-vis spectroscopy report

Figure 2(a) indicates the UV-vis spectrum of pristine Au NP in toluene solvent. A peak at  $520\text{ nm}$  confirmed the presence of Au NP.<sup>26</sup> The AM decorated Au NP is appeared at  $544\text{ nm}$  [Fig. 2(b)]. The red shift in peak position confirmed the existence of strong interaction between Au NP and AM through S atom. The UV-vis spectrum of PNIPAAm-AM-Au system is shown in Figure 2(c). This system showed one new peak at  $679\text{ nm}$ , corresponding to the longitudinal surface plasmon peak and the absorption peak position of the same decreased with the decrease in aspect ratio of Au nanorod.<sup>27</sup> A longitudinal plasmon absorption peak at  $679\text{ nm}$  indicates that the Au nanorods are having low aspect ratio. This study infers that during the *in situ* polymerization process, the nanosphere form of Au is converted into nanorod form of Au (i.e.) internal conversion of sphere into rod form. Figure 2(d) confirmed the TEM image of pristine Au nanoparticle. The Au nanoparticles are having the diameter of  $10\text{--}20\text{ nm}$ . Generally, the Au nanorods are prepared through the seed assisted method; the present investigation produced an alternate method for the synthesis of Au nanorod easily and economically.

#### PLS study

The photoluminescence spectrum (PLS) of PNIPAAm-AM-Au system is shown in Figure 3. It shows an emission peak at  $675\text{ nm}$ , and the intensity of the same is increased with the increase of excitation energy level. The excitation energy was varied from  $375$  to  $445\text{ nm}$ ; thereafter, it showed a decreasing trend (the decreasing trend is not shown in





**Figure 3** PLS of PNIPAAm-AM-Au system excited at (a) 375 nm, (b) 390 nm, (c) 410 nm, (d) 420 nm, and (e) 445 nm.

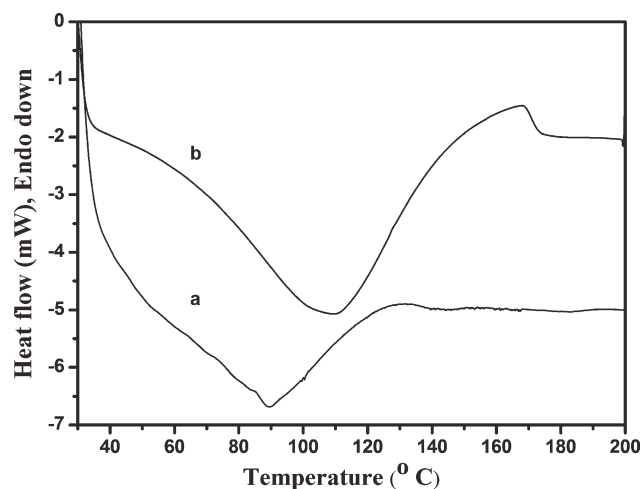
Fig. 3). Figure 3(a–e) indicates the PLS of Au nanorod excited at different energy levels. Although increasing the excitation energy level, the intensity was varied from 1 to 5.5 cps. This indicates that the Au nanorod form is stable up to a wide a range of input energy level. The PLS of Au nanorod was explained by Montalti et al.<sup>28</sup> and Liao et al.<sup>29</sup> In comparison with the literature value, there is not that much difference in the PL value.

#### DSC profile

The DSC heating scan of PNIPAAm is shown in Figure 4(a). It shows one broad endothermic peak at 88.6°C due to the removal of physisorbed water molecules (i.e.) dewatering temperature ( $T_{d,w}$ ) and one-step down-like transition, due to glass transition temperature ( $T_g$ ), appearing at 139.8°C. The PNIPAAm-AM-Au system [Fig. 4(b)] also exhibits the same type of transitions at 109.8 and 175.1°C due to the  $T_{d,w}$  and  $T_g$ , respectively. In comparison, the PNIPAAm-AM-Au system showed higher  $T_g$  and  $T_{d,w}$  values than the pristine PNIPAAm. The increase in  $T_{d,w}$  and  $T_g$  confirmed the copolymerization nature of NIPAAm with Au-AM monomer. The pristine PNIPAAm showed the  $T_g$  value of 135°C.<sup>30</sup> Recently, Alli and research team<sup>31</sup> investigated the multiple  $T_g$  with decreasing trend while PNIPAAm was crosslinked with soybean oil and polypropylene glycol. The present investigation exhibits the improved  $T_g$  value than the literature value.

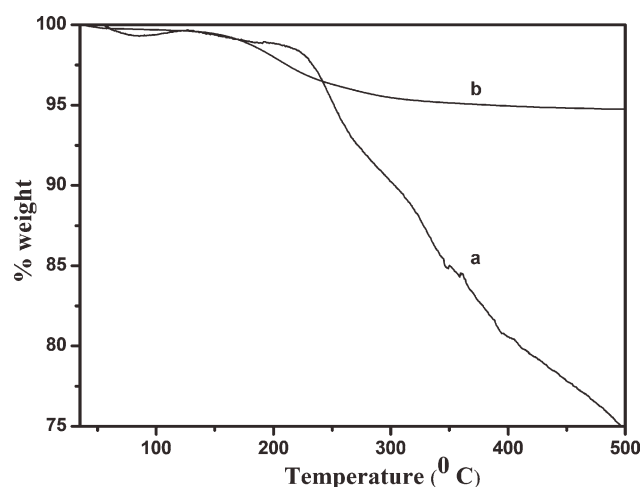
#### TGA history

Figure 5(a) exhibits the thermogravimetric analysis (TGA) thermogram of PNIPAAm. It shows a two-step degradation process. The first, minor weight



**Figure 4** DSC of (a) PNIPAAm and (b) PNIPAAm-AM-Au.

loss step at 88.3°C is due to the removal of physisorbed water molecules from PNIPAAm. This supported the FTIR spectrum [Fig. 1(a)] and DSC heating scan [Fig. 4(a)] of PNIPAAm. The second, major weight loss step at 218°C is associated with the dissociation of intermolecular hydrogen bonding of PNIPAAm backbone. Above 450°C, it showed 75% weight residue remain. This confirmed the thermal stability of PNIPAAm. Figure 5(b) indicates the TGA thermogram of PNIPAAm-AM-Au system. The system shows a single-step degradation process around 200°C, due to the breaking of intermolecular forces between PNIPAAm chains. Above 450°C, it showed 95% weight residue remain. The thermal stability of PNIPAAm copolymers was compared to the literature report<sup>16</sup> and the present system produced an excellent result. Although comparing the thermal stability of PNIPAAm and PNIPAAm-AM-Au systems, the later one exhibited the higher thermal



**Figure 5** TGA of (a) PNIPAAm and (b) PNIPAAm-AM-Au.

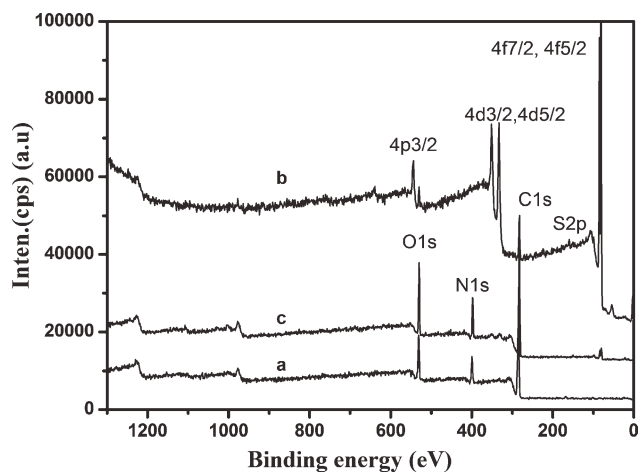


**Figure 6** XPS of (a) PNIPAAm, (b) AM decorated Au NP, and (c) PNIPAAm-AM-Au.

stability due to the copolymerization as well as crosslinking nature of Au-AM monomer.

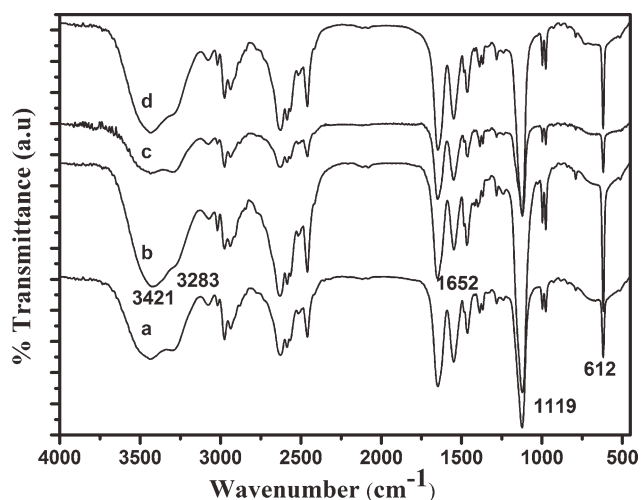
#### XPS analysis

Figure 6(a) indicates the X-ray photoelectron spectroscopy (XPS) of PNIPAAm. The C1s, N1s, and O1s peaks are appeared at 530.8, 389.1, and 282.8 eV, respectively. Figure 6(b) shows the XPS of AM decorated Au NP. A twin peak around 83 eV confirmed the presence of  $4f_{7/2}$  and  $4f_{5/2}$  energy level of Au NP.<sup>32</sup> The  $4P_{3/2}$ ,  $4d_{3/2}$ , and  $4d_{5/2}$  energy level of Au NP is observed at 546.3, 348.7, and 329.5 eV, respectively. The C1s and S2p energy level of AM is observed at 283.07 and 158.9 eV, respectively. Appearance of  $4f_{5/2}$  and  $4f_{7/2}$  peaks confirmed that the Au is in  $Au^0$  state. Moreover, the sulfur region exhibits a singlet peak at 158.9 eV, showing the existence of S on the surface of Au NP. Thus, the XPS confirmed the AM decorated Au NP. Figure 6(c) indicates the XPS of PNIPAAm-AM-Au system. Peaks due to Au- $4f_{7/2}$ ,  $4f_{5/2}$ , S2p, C1s, N1s, and O1s are observed, which confirmed the presence of AM decorated Au NP in PNIPAAm matrix as a comonomer.

#### Synthesis and characterizations of MWCNT-AA-PNIPAAm

##### FTIR spectrum

Figure 7(a) indicates the FTIR spectrum of pristine poly(*N*-isopropyl acrylamide) (PNIPAAm). The important peaks are already characterized. Figure 7 (b-d) indicates the FTIR spectrum of multiwall carbon nanotube (MWCNT), OMWCNT, and AA-MWCNT-bound PNIPAAm, respectively. In these systems, also the above said peaks were observed. Specific



**Figure 7** FTIR spectra of (a) PNIPAAm, (b) PNIPAAm-MWCNT, (c) PNIPAAm-OMWCNT, (d) PNIPAAm-AA-MWCNT.

peaks corresponding to MWCNT are not observed here.

##### DSC study

The DSC heating scan of PNIPAAm is given in Figure 8(a). The heating scan was varied from room temperature to 175°C. It shows one endothermic peak at 82°C, due to the  $T_{d,w}$ . The DSC heating scan of PNIPAAm-MWCNT is shown in Figure 8(b). The heating scan exhibits one hump at 84.5°C, due to  $T_{d,w}$ . The broadening of the  $T_{d,w}$  was suppressed due to the influence of hydrophobic MWCNT dispersion. Here, the  $T_g$  was broadened and decreased to 127.9°C due to the hydrophobic MWCNT dispersion on the PNIPAAm matrix and also due to the possible intercalation of PNIPAAm chains into the

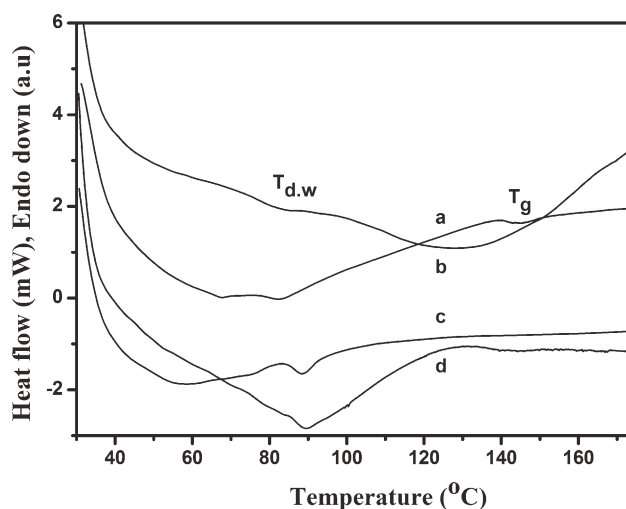


**Figure 8** DSC of (a) PNIPAAm, (b) PNIPAAm-MWCNT, (c) PNIPAAm-OMWCNT, and (d) PNIPAAm-AA-MWCNT.

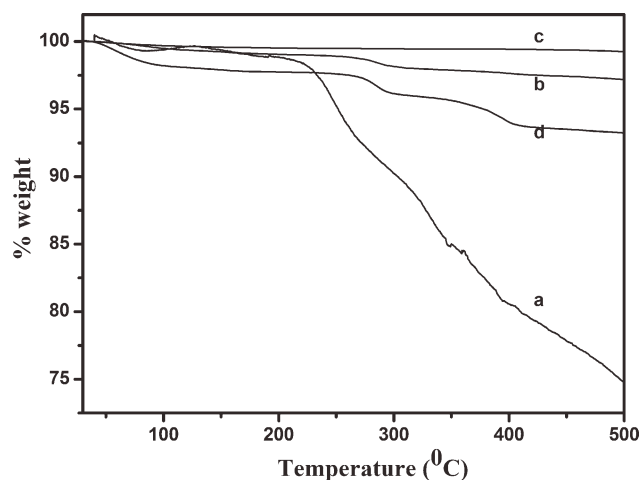


**Figure 9** TGA of (a) PNIPAAm, (b) PNIPAAm-MWCNT, (c) PNIPAAm-OMWCNT, (d) PNIPAAm-AA-MWCNT.

layered arrangement of MWCNT. The PNIPAAm-OMWCNT [Fig. 8(c)] and PNIPAAm-AA-MWCNT [Fig. 8(d)] systems show the  $T_{d,w}$  at 88.3 and 89.7°C, respectively. The PNIPAAm-OMWCNT system did not show the  $T_g$  (i.e.) the system is not having  $T_g$ . This is due to the thorough mixing of OMWCNT with the PNIPAAm matrix. The  $T_g$  of PNIPAAm-AA-MWCNT system was appeared at 143.9°C. In the case of OMWCNT, the possible hydrogen bonding explained the increase in  $T_{d,w}$ . In the case of AA-MWCNT, copolymerization and crosslinking of AA-MWCNT and NIPAAm monomers explained the increase in  $T_{d,w}$ . The DSC study inferred that the copolymerization increased the  $T_{d,w}$  of PNIPAAm. In 2004, Kong et al.<sup>33</sup> explained the DSC of PNIPAAm-coated carbon nanotubes. Our reports coincided with the results of Kong and coworkers.<sup>33</sup>

#### TGA analysis

The thermogravimetric analysis (TGA) thermogram of PNIPAAm is given in Figure 9(a) and already thoroughly discussed. The PNIPAAm-MWCNT system [Fig. 9(b)] shows a two-step degradation process. The first, minor weight loss step below 100°C is due to the removal of moisture and  $T_{d,w}$ . This supported the FTIR spectrum (OH stretching) and DSC results ( $T_{d,w}$ ). The second, major weight loss step around 280°C is corresponding to the dissociation of PNIPAAm intermolecular forces. Above 450°C, it exhibited 97% weight residue remain. The increase in thermal stability is due to the covering of PNIPAAm chains by the MWCNT<sup>33</sup> (similar to umbrella effect). Figure 9(c) represents the TGA thermogram of PNIPAAm-OMWCNT system. This system shows a two-step degradation process. As usual, the first, minor weight loss step is due to the loss of moisture and physisorbed water molecules. The sec-

ond, minor weight loss step around 450°C is due to the PNIPAAm backbone degradation. Above 450°C, it showed 99.2% weight residue remain. When compared with the pristine PNIPAAm and PNIPAAm-MWCNT systems, the present system yielded a highest thermal stability. Figure 9(d) shows the TGA thermogram of PNIPAAm-AA-MWCNT. The thermogram exhibits a three-step degradation process. The first, minor weight loss below 200°C is due to the removal of moisture and water molecules. The second, minor weight loss around 280°C is associated with the dissociation of intermolecular forces (hydrogen bonding between PNIPAAm chains). The third, minor weight loss step around 380°C is responsible for the degradation of PNIPAAm chains. Above 450°C, it showed 93.3% weight residue remain. In comparison, the PNIPAAm-OMWCNT system showed the higher thermal stability due to the strong secondary forces of attraction like hydrogen bonding. In the FTIR spectrum of PNIPAAm-OMWCNT [Fig. 7(c)], a broad widened peak was observed around 3500–3250  $\text{cm}^{-1}$ , and this explained the (merging of) intermolecular hydrogen bonding forces between the *N*-isopropyl group of PNIPAAm and carboxyl group of OMWCNT.

#### XPS report

Figure 10(a) indicates the X-ray photoelectron spectroscopy (XPS) of PNIPAAm with C1s, O1s, and N1s peaks<sup>34</sup> and already discussed. The same types of peaks were observed for PNIPAAm-MWCNT (Fig. 10b), PNIPAAm-OMWCNT [Fig. 10(c)], and PNIPAAm-AA-MWCNT [Fig. 10(d)] also. There is no change in the peak position. In 2006, Xu et al.<sup>34</sup> reported the higher binding energy for the PNIPAAm-MWCNT system. Other research teams also

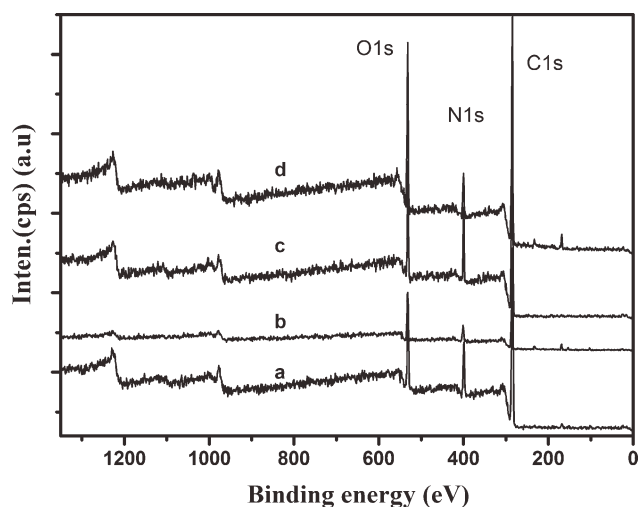


**Figure 10** XPS of (a) PNIPAAm, (b) PNIPAAm-MWCNT, (c) PNIPAAm-OMWCNT, and (d) PNIPAAm-AA-MWCNT.

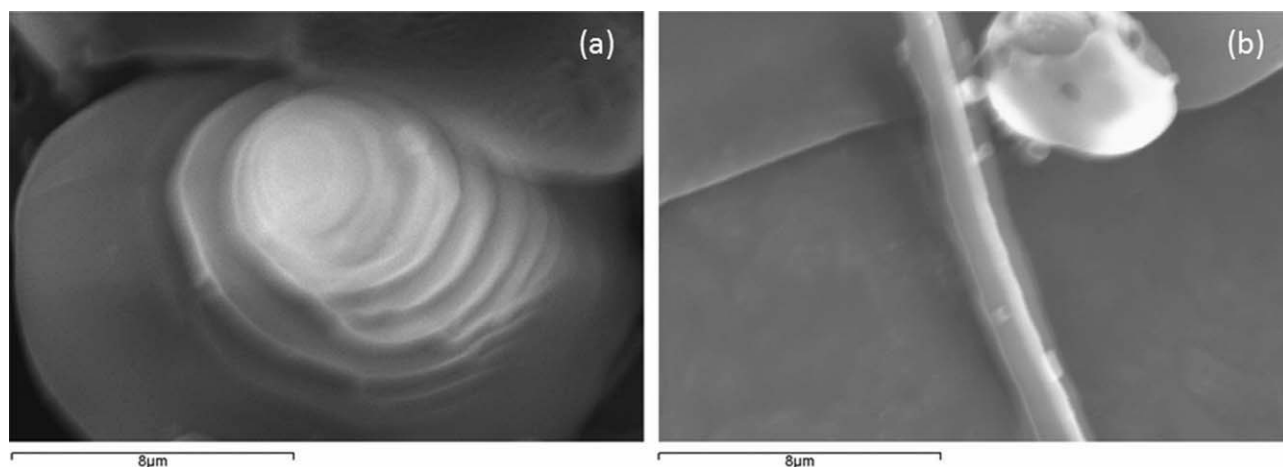


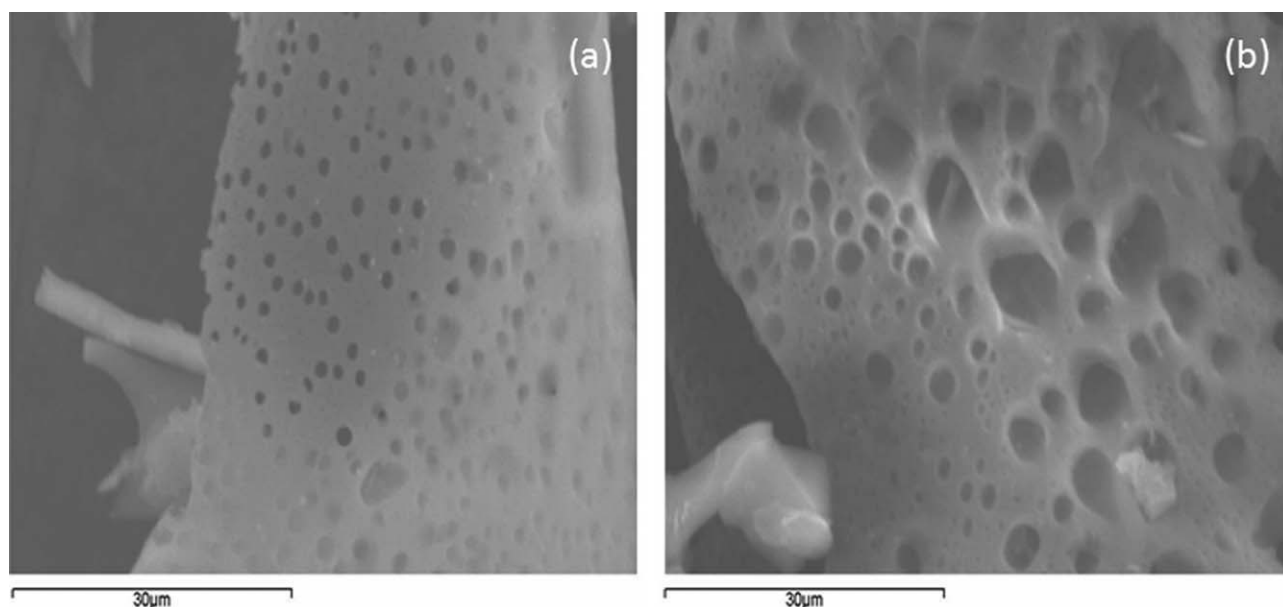
**Figure 11** SEM of PNIPAAm with (a) rose flower like morphology and (b) rodlike morphology.

reported about the binding between PNIPAAm and with different MWCNTs<sup>35–38</sup> through XPS analysis. Our reports coincided with the results of Zhang et al.<sup>36</sup>

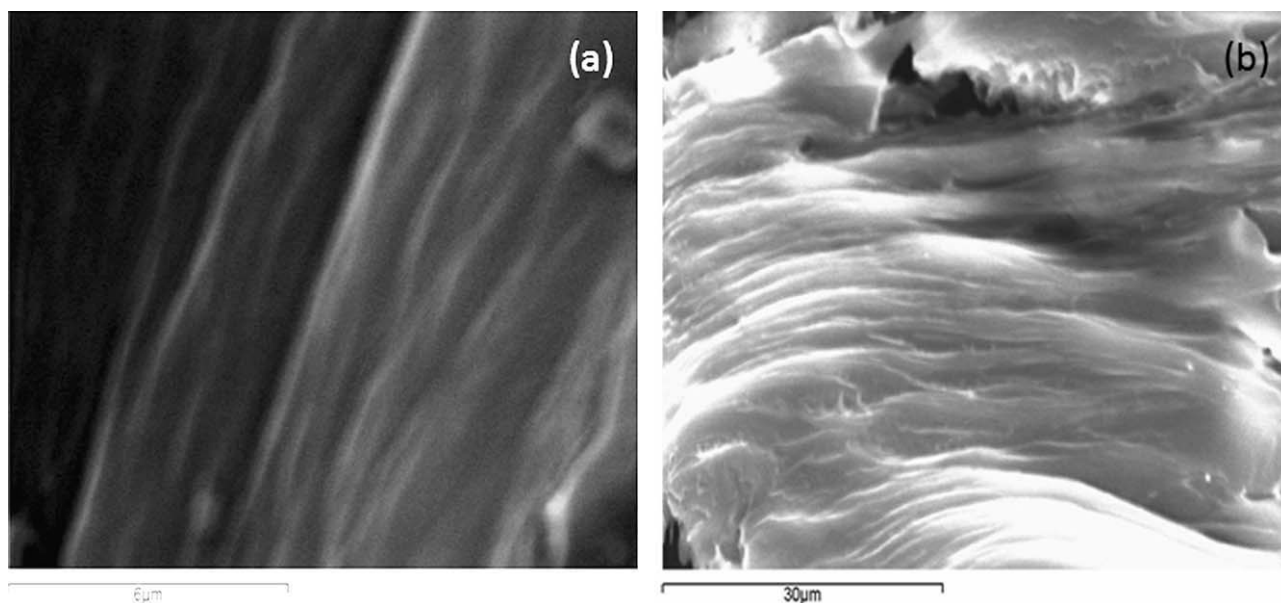
#### SEM analysis

Figure 11(a) indicates the scanning electron microscopy (SEM) morphology of pristine PNIPAAm. It shows a rose flower-like soft morphology. Figure 11(b) shows the microrod-like morphology with micropores on the surface. Appearance of micropores is the peculiar character of the materials for the drug-delivery applications. The voids or micropores on the polymer backbone provide a space for the accommodation of drugs during the drug-loading process. After the drug-delivery process, again

the micropores are re-appeared. Meanwhile, at a suitable pH, the polymer itself can be degraded through hydrolysis reaction. In such a way, the PNIPAAm is a suitable candidate for the drug-delivery applications. Although adding the AA-MWCNT to the NIPAAm monomer during the *in situ* polymerization process, more micropores were produced on the surface of PNIPAAm [Fig. 12(a)]. Figure 12(b) confirms the insertion of AA-MWCNT into the micropores of the PNIPAAm. Although adding OMWCNT to the NIPAAm monomer during the *in situ* polymerization process, the surface morphology was completely changed. MWCNTs are observed with the approximate length of 15  $\mu\text{m}$  with the breadth of 150 nm [Fig. 13(a)]. This indicated that the layered MWCNTs were hanged in the micropores of PNIPAAm during the *in situ*



**Figure 12** SEM of PNIPAAm-AA-MWCNT without (a) and with (b) the insertion of AA-MWCNT into the micropores of PNIPAAm.



**Figure 13** SEM of PNIPAAm-OMWCNT system (a) with the dispersion of OMWCNT on the PNIPAAm surface and (b) rough surface of PNIPAAm.

polymerization reaction. Figure 13(b) indicates the fiber-like morphology with lesser number of micropores on the surface of PNIPAAm. This is due to the existence of good chemical interaction between OMWCNT and PNIPAAm matrix.

### CONCLUSIONS

From the above study, the important points are summarized here as conclusions. (1) The FTIR spectrum confirmed the metal-sulfide ( $675\text{ cm}^{-1}$ ) linkage in the PNIPAAm-AM-Au system. (2) The PNIPAAm-AM-Au system exhibited the higher  $T_g$  ( $172^\circ\text{C}$ ) than the pristine PNIPAAm ( $135.7^\circ\text{C}$ ) due to the copolymerization and crosslinking reactions. (3) The  $T_{d,w}$  of PNIPAAm-AA-MWCNT was greater than that of pristine PNIPAAm due to the copolymerization reaction. (4) The PL intensity of PNIPAAm-AM-Au was increased with the increase of excitation energy level up to 445 nm. (5) The UV-vis spectrum of PNIPAAm-AM-Au system exhibited a peak at 679 nm corresponding to the Au nanorod form. (6) The TGA declared the higher thermal stability for to the PNIPAAm-AM-Au and PNIPAAm-AA-MWCNT systems due to the copolymerization reaction. (7) XPS confirmed the appearance of  $4f_{7/2}$  and  $4f_{5/2}$  energy levels due to the zero oxidation state of Au.

### References

- da Silva, R. M. P.; Mano, J. F.; Reis, R. L. *Trends Biotechnol* 2007, 25, 577.
- Vanga, J.; Janovak, L.; Vanga, E.; Dekany, I.; Kemeny, L. *Skin Pharmacol Physiol* 2009, 22, 305.
- Jun, L.; Bochu, W.; Yazhou, W. *Int J Pharmacol* 2006, 2, 513.

- Zhou, R. X.; Li, W. *J Polym Sci Part A: Polym Chem* 2003, 41, 152.
- Yan, H.; Tsujii, K. *Colloids Surf B Biointer* 2005, 46, 142.
- Stile, R. A.; Burghardt, W. R.; Healy, K. E. *Macromolecules* 1999, 32, 7370.
- Malonne, H.; Eeckman, F.; Fomtaine, D.; Amighi, K. *Eur J Pharm Biopharm* 2005, 61, 188.
- Tasdelen, B.; Apohan, N. K.; Misirili, Z.; Guven, O.; Baysal, B. M. *J Appl Polym Sci* 2005, 97, 1115.
- Wu, X. S.; Hoffman, A. S.; Yager, P. *J Polym Sci Part A: Polym Chem* 1992, 30, 2121.
- Chen, Q.; Xu, K.; Zhang, W.; Song, C.; Wang, P. *Colloid Polym Sci* 2009, 287, 1339.
- Erbil, C.; Kazancioglu, E.; Yanamik, N. *Eur Polym J* 2004, 40, 1145.
- Zhang, Y. X.; Fang, Q.; Fu, Y. Q.; Da, A. H.; Esch, T. E. H. *Polym Int* 2000, 49, 763.
- Ju, X. J.; Chu, L. Y.; Zhu, X. L.; Chen, W. M. *Smart Mater Struct* 2006, 15, 1767.
- Huh, K. M.; Harshi, J.; Ooya, T.; Yui, N. *Mater Chem Phys* 2000, 201, 619.
- Frimpong, R. A.; Hilt, J. Z. *Nanotechnology* 2008, 19:175101.
- Pierson, R.; Basavaraja, C.; Kim, N. R.; Jo, E. A.; Huh, D. S. *Bull Kor Chem Soc* 2009, 30, 2057.
- Choi, C. Y.; Kim, T. H.; Kim, D. G.; Nah, J. W. *Appl Chem* 2004, 8, 430.
- Xiao, X. C. *Expr Polym Lett* 2007, 1, 232.
- Renfer, M.; Leyra, P. D.; Lynch, I.; Scheffold, F. *Eur Phys J E* 2009, 28, 165.
- Sousa, A. D.; Maria, D. A.; Sousa, R. G. D.; Sousa, E. M. B. D. *J Mater Sci* 2010, 45, 1478.
- Gilanyi, T.; Varga, I.; Mezaros, R.; Filipsei, G.; Zrinyi, M. *Phys Chem Chem Phys* 2000, 2, 1973.
- Allan, M. A.; Miah, M. A. J.; Ahmad, H. *J Appl Sci* 2008, 8, 352.
- Xu, G. Y.; Wu, W. T.; Wang, Y.; Pang, W.; Wang, P. *Nanotechnology* 2007, 18, 145606.
- Shi, J.; Alves, N. M.; Mano, J. F. *Macromol Biosci* 2006, 6, 358.
- Haragudhi, K.; Xu, Y.; Li, G. *Macromol Rapid Commun* 2010, 31, 718.

26. Saha, B.; Bhattacharya, J.; Mukherjee, A.; Dasgupta, A. K.; Kar-makar, P. *Nanoscale Res Lett* 2007, 2, 614.
27. Sharma, V.; Park, K.; Srinivasarao, M. *PNAS* 2009, 106, 4981.
28. Montalti, M.; Prodi, L.; Zaccheroni, N.; James, S. L. *J Am Chem Soc* 2007, 129, 2418.
29. Liao, H.; Wen, W.; Wong, W. K. L. *J Opt Soc Am B* 2006, 23, 2518.
30. Sousa, R. G.; Magalhaes, W. F.; Freitas, R. F. S. *Polym Deg Stab* 1998, 61, 275.
31. Alli, A.; Hazer, B. *Eur Polym J* 2008, 44, 1701.
32. Whyman, R. *J Chem Soc Chem Commun* 1994, 801.
33. Kong, H.; Li, W.; Yan, D.; Kroto, H. W. *Macromolecules* 2004, 37, 6683.
34. Xu, G.; Wu, W. T.; Wang, Y.; Pang, W.; Wang, P.; Zhu, Q.; Liu, F. *Nanotechnology* 2006, 17, 2458.
35. Yang, D.; Guo, G.; Hu, J.; Wang, C.; Jiang, D. *J Mater Chem* 2008, 18, 350.
36. Zhang, C.; Easteal, A. J. *J Appl Polym Sci* 2007, 104, 1723.
37. You, Y. Z.; Hong, C. Y.; Pan, C. Y. *Adv Funct Mater* 2007, 17, 2470.
38. Liu, Y. Z.; Chen, W. H. *Macromolecules* 2007, 40, 8881.